

2. Fabrication of circular slot antennas

Figure 1(a) and (b) show the cross-sectional and plain views of circular slot antennas fabricated on ALD-made $\text{Al}_2\text{O}_3/\text{SiC}$. ALD was performed using trimethylaluminum (TMA) and H_2O along with commercially-available equipment. The thicknesses of the Al_2O_3 layers were varied from 0 to 100 nm. Next, circular slot antenna patterns were made by electron-beam lithography. Then, Au (40 nm)/Ti (10 nm) were deposited on the substrate, followed by a lift-off technique that cut out circular openings in the metal sheet. One antenna array consisted of 10 x 10 elements, each having the same size. The diameter of the circles was 3 to 6 μm . The distance of the adjacent antennas was 9 μm . The reflection spectra were measured with a micro FTIR without a polarizer, and the normalized reflectivity was obtained using the spectrum from Au.

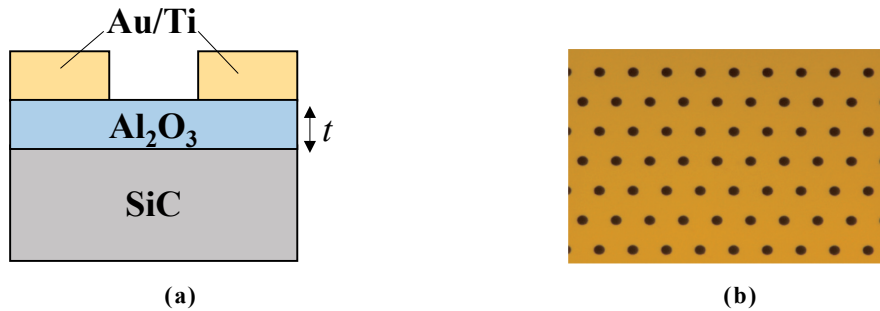


Fig. 1 (a) Cross-sectional view of a circular slot antenna fabricated on $\text{Al}_2\text{O}_3/\text{SiC}$ and (b) Plain view of antenna array.

3. Results and discussions

Figure 2 shows the results for the normalized reflectivity of antenna arrays with the thickness, t , of Al_2O_3 being changed. The diameter of the antenna was 6 μm . When $t = 0$ nm, it was found that a decrease in reflectivity at 929 cm^{-1} , caused by SPhP, appeared among the Reststrahlen band of SiC ranging from 800 to 970 nm. This dip almost disappeared when $t = 100$ nm, because the interface of Al_2O_3 and SiC was distant from the antenna, and field enhancement was weak. However, looking closer, one notices that the decrease in reflectivity due to SPhP signals was not monotonously reduced with the Al_2O_3 thickness, which is shown in Fig. 3(a). There, the dip depth was measured with reference to that of $t = 0$ nm. It was 85% at

$t = 5$ nm, and increased to 90% at $t = 10$ nm. The dip was smaller as t was increased over 10 nm.

Generally, as t increases, the intensity of electric fields perpendicular to the substrate surface, E_z , should be at maximum. This is easily anticipated from the following: although E_z is zero on the surface of the substrate, it starts to appear distant from the surface. E_z eventually vanishes at a great distance, thereby leading to the existence of a peak at a certain position distant from the surface. In this case, further account must be taken into the absorption in Al_2O_3 . The relationship between absorption coefficient α and extinction coefficient κ is represented by $\alpha = 4\pi\kappa / \lambda$. κ of ALD- Al_2O_3 was measured by an ellipsometer and was 0.574 at 932 cm^{-1} , which was different from the data in Ref. [3]. When this value was used, α

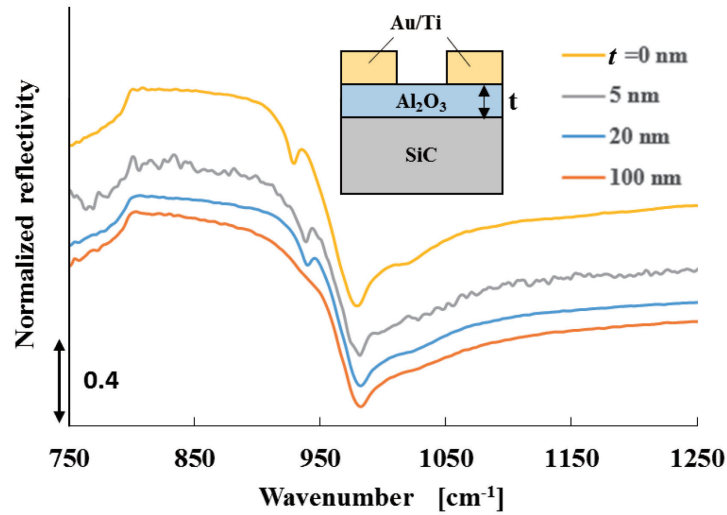


Fig. 2 Normalized reflectivity of circular-slot antenna array on $\text{Al}_2\text{O}_3/\text{SiC}$ substrate when the thickness of Al_2O_3 was changed.

became $6.78 \times 10^{-4} \text{ nm}^{-1}$. On the assumption that the Beer-Lambert law and no enhancement of electric field by the antenna, $|E_z|^2$ attenuated to 0.997 when t was 5 nm, meaning that there was only a 0.3% decrease. However, the results are different in the cases where an antenna is present. Namely, equivalent thickness of Al_2O_3 should grow due to enhanced electric field, increasing considerable attenuation of input light as it propagates into Al_2O_3 . Figure 3(b) shows the results of FDTD calculation of enhancement of $|E_x|^2$ and $|E_z|^2$ vs. Al_2O_3 thickness, which

was made near the edge of Au. Enhancement of $|E_z|^2$ was 45, when $t = 0$ nm, which was reasonably in agreement with the result shown in Fig. 3(a).

Next, the phase was calculated of the structure for air/SiC (i. e. $t = 0$ nm) based on the equation, $k_{SPhP}D + \varphi = 2\rho_{m,n}$. Here, k_{SPhP} is the SPhP wavenumber parallel to the substrate surface, φ is the phase change upon the circular edge, and $\rho_{m,n}$ is the m th zero point of the n th Bessel function. Moreover, k_{SPhP} was obtained calculating the dispersion characteristics for the air/SiC and using measured wavenumber of

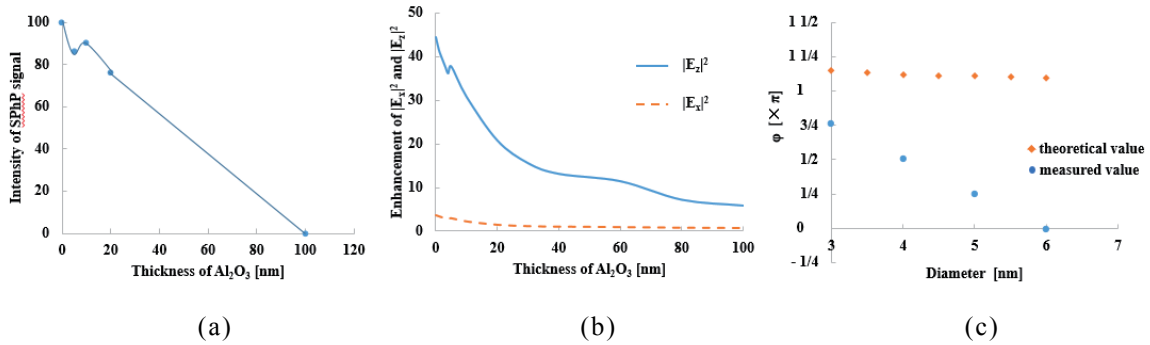


Fig. 3 (a) SPhP signal intensity vs. the thickness of Al₂O₃ layer, (b) Enhancement of $|E_x|^2$ and $|E_z|^2$ with FDTD simulation, and (c) Phase dependence on diameter.

SPhP ($= 932 \text{ cm}^{-1}$). Phase dependence on diameter is shown in Fig. 3(c), indicated as a measured value where $m = 1$ and $n = 0$ were assumed. Calculation of φ from the imaginary part of the complex reflection coefficient r_m [4] was also conducted, indicating it as the theoretical value in Fig. 3(c). There is a difference coming out of two calculation approaches, and there is a room for examination.

4. Conclusion

Distribution of electric fields perpendicular to the antennas increased by circular slot antennas was investigated by monitoring SPhP signals. When the thickness of the Al₂O₃ layer was 100 nm, the SPhP signal almost disappeared. The result that the electric fields enhanced by antennas hardly existed at a depth of 100 nm.

Acknowledgement

This work was supported by JSPS KAKENHI Grant Number 23560043, and Nano-Integration Foundry (NIMS) in "Nanotechnology Platform Project" operated by the Ministry of Education, Culture, Sports, Science and Technology (MEXT), Japan.

References

- [1] Miyata, J. et al., in *ANNIC2015*, Paris, France (2015).
- [2] Wang, T. et al., *Nano Lett.* **13**, 5051-5055 (2013).
- [3] Palik, E.D., *Handbook of Optical Constants of Solids II*, San Diego: Academic Press (1991).
- [4] Filter, R. et al., *Phys. Opt.* **85**, 1-16 (2012).